J. Fluid Mech. (2007), *vol.* 584, *pp.* 415–431.
doi:10.1017/S0022112007006623 Printed in the United Kingdom

Gravity currents over fractured substrates in a porous medium

DAVID PRITCHARD

Department of Mathematics, University of Strathclyde, 26 Richmond Street, Glasgow G1 1XH, UK
dtp@maths.strath.ac.uk

(Received 27 February 2006 and in revised form 21 March 2007)

We consider the behaviour of a gravity current in a porous medium when the horizontal surface along which it spreads is punctuated either by narrow fractures or by permeable regions of limited extent. We derive steady-state solutions for the current, and show that these form part of a long-time asymptotic description which may also include a self-similar 'leakage current' propagating beyond the fractured region with a length proportional to $t^{1/2}$. We discuss the conditions under which a current can be completely trapped by a permeable region or a series of fractures.

1. Introduction

There are many geological situations in which fluid spreads through a layered porous medium. Important examples of such systems include aquifers and oil or geothermal reservoirs (see e.g. Bear 1972), and the flows may be natural or artificial: examples of the latter include waterflooding in an oil reservoir (Latil 1980) and the sequestration of carbon dioxide or other pollutants in saline aquifers (Bachu 2000; Nordbotten, Celia & Bachu 2004; Bickle *et al.* 2007). In many instances, the fluid spreads laterally along an impermeable or almost impermeable layer in the medium, driven by the buoyancy contrast between it and the ambient fluid: the resulting flows are generally known as gravity currents. The theory of such flows is well developed, and a particularly useful technique in their investigation has been to develop models, in the form of nonlinear diffusion equations, which admit self-similar solutions. These self-similar solutions then describe the asymptotic behaviour of the flow as it spreads far from its initial injection point or beyond its original spatial distribution (see e.g. Barenblatt 2003, chapter 2).

When the layer along which the fluid spreads is not quite impermeable, the current may lose mass by drainage through this layer, and in this situation the usual self-similar solutions are no longer valid. Indeed, the current may exhibit behaviour such as spatially limited spreading which cannot be described by similarity solutions. The first study of how this drainage might affect the spreading of a gravity current in a porous medium was carried out by Pritchard, Woods & Hogg (2001), hereafter PWH01, who investigated drainage, driven by hydrostatic pressure, through a thin, spatially uniform underlying layer. For releases of a constant volume of fluid, PWH01 found a class of exact solutions which were not self-similar but which were attracting under most conditions; when fluid is injected at a constant rate, the attracting solutions of the system are steady solutions characterized by a local balance between drainage and the supplied flux. Almost simultaneously with PWH01, Acton, Huppert &

Worster (2001) obtained analogous results for a viscous gravity current spreading over and draining into a porous medium. The model of PWH01 was later extended by Pritchard & Hogg (2002), who considered a more general model for the drainage rate, and by King & Woods (2003), who developed a class of 'dipole' solutions for currents which drain both vertically through an underlying layer and backwards through the point of injection. A more distant but interesting parallel is provided by models of currents which lose mass through capillary retention (Barenblatt 2003, chapter 3), or through evaporation (Woods 1998).

Almost all the theoretical work on the effect of drainage on gravity currents has treated a spatially distributed mass loss term. However, this is not a good model for all geological systems. In many formations, we may expect the low-permeability layers to be inhomogeneous in thickness and composition, and in the extreme case, they may be discontinuous or fractured. When a current spreads along a fractured substrate, its spreading will be controlled by the rate at which fluid is lost through the individual fractures, the spatial scale of which may be much less than that of the current itself. This provides a natural complement to the case of distributed drainage considered by PWH01 and others, and it is this situation which we consider in the current study. Our emphasis will be on determining when a current can be completely trapped by the fractured substrate and prevented from propagating further, and if it can propagate beyond the fractured region, how its propagation is affected.

In § 2 we describe the model which we will employ. In § 3 we describe the flow which results when the current encounters a single isolated fracture. In § 4 we consider the effect of a series of discrete fractures or a continuous but finite permeable region in the substrate. We summarize our results and draw some conclusions in § 5.

2. Description of the discrete-fracture model

We consider a layer of buoyant fluid spreading unidirectionally in a deep porous layer, along a horizontal caprock. The caprock is taken to be generally impermeable, but to contain occasional line fractures perpendicular to the direction of flow. These line fractures are narrow compared to the streamwise length scale of the flow, and so act in a two-dimensional model as point sinks of fluid; we will discuss this 'point sink' assumption below. Throughout, we will make the shallow-flow approximation that, except in the immediate vicinity of a fracture, the horizontal length scale of the current is much greater than its depth. This allows us to treat the pressure in the current as hydrostatic and the velocity as horizontal (Huppert & Woods 1995).

Away from the fractures, the fluid spreads under gravity according to

$$\frac{\partial \hat{h}}{\partial \hat{t}} = \hat{\beta}\frac{\partial}{\partial \hat{x}}\left(\hat{h}\frac{\partial \hat{h}}{\partial \hat{x}}\right), \qquad \text{where} \qquad \hat{\beta} = \frac{\hat{K}\hat{g}\Delta\hat{\rho}}{\hat{\mu}\phi} \tag{2.1}$$

(see e.g. Huppert & Woods 1995). Here $\hat{h}(\hat{x},\hat{t})$ is the fluid depth, ϕ and $\hat{K}$ are the porosity and permeability of the porous layer, $\Delta\hat{\rho} > 0$ is the density contrast between the injectate and the ambient fluid and $\hat{\mu}$ is the viscosity of the injectate. (Note that the parameter $\hat{\beta}$ has the dimensions of velocity: throughout, we will denote dimensional variables by a caret, while dimensionless variables are unadorned.)

We take the ith fracture to have streamwise width $\hat{W}_i$, porosity ϕ_i and effective permeability $\hat{K}_i$; the caprock layer is presumed to have thickness $\hat{b}$, and we assume that it is sufficiently thin that the fracture saturates effectively instantaneously. The

rate of loss of volume per unit width from the current is then given by

$$\hat{q}_i = \hat{v}_i \hat{W}_i \equiv \hat{\lambda}_i \hat{h}(\hat{x}_i), \qquad \text{where} \qquad \hat{v}_i = \frac{\hat{K}_i}{\hat{\mu}} \frac{\Delta \hat{\rho} \hat{g} \hat{h}}{\hat{b}} \quad \text{and} \quad \hat{\lambda}_i = \frac{\hat{K}_i}{\hat{\mu}} \frac{\Delta \hat{\rho} \hat{g} \hat{W}_i}{\hat{b}}. \tag{2.2}$$

(The derivation and validity of this drainage rate have been discussed by PWH01 and by Pritchard & Hogg 2002.) The conservation of fluid volume therefore gives

$$\left[\hat{h} \frac{\partial \hat{h}}{\partial \hat{x}} \right]_{\hat{x}_{i-}}^{\hat{x}_{i+}} = \hat{\lambda}_i \hat{h}(\hat{x}_i, \hat{t}) \qquad \text{at each point} \quad \hat{x} = \hat{x}_i. \tag{2.3}$$

We will consider currents which are fed at $\hat{x} = 0$ by a constant volume flux per unit width $\hat{q}$, so

$$-\hat{\beta} \hat{h} \frac{\partial \hat{h}}{\partial \hat{x}} = \hat{q} \qquad \text{at} \qquad \hat{x} = 0. \tag{2.4}$$

2.1. *Validity of the point sink model*

The key assumption of the 'point sink' model is that the shallow-flow assumptions are violated (i.e. two-dimensional flow occurs) only near the fracture, in a region which is of small horizontal extent relative to the current. Such local violations are common in models of viscous and porous-medium gravity currents, near either the point of injection (e.g. Lyle *et al.* 2005) or the flow front (e.g. Huppert 1982), and these examples suggest that local violation does not invalidate the rest of the solution. We may therefore be reasonably confident of our approach as long as the two-dimensional flow region is indeed small.

From the continuity equation, we deduce that if the two-dimensional flow induced by a fracture varies over a length scale $\hat{L}$, we must have $\hat{u}/\hat{L} \sim \hat{v}/\hat{h}$. Again by continuity, we may estimate $\hat{v}$ by the drainage velocity in the fracture, $\hat{v} \sim \hat{v}_i = \hat{\lambda}_i \hat{h}/\hat{W}_i$; meanwhile we may estimate $\hat{u}$ by dividing the flux arriving at the fracture by the depth, $\hat{u} \sim \hat{q}_i/\hat{h}$. Hence

$$\frac{\hat{q}_i}{\hat{h}\hat{L}} \sim \frac{\hat{\lambda}_i \hat{h}}{\hat{W}_i \hat{h}}, \qquad \text{i.e.} \qquad \hat{L} \sim \frac{\hat{q}_i}{\hat{h}} \frac{\hat{W}_i}{\hat{\lambda}_i}. \tag{2.5}$$

We will see below that the system favours states in which $\hat{h}(x_i) \sim \hat{q}_i/\hat{\lambda}_i$, and so we have $\hat{L} \sim \hat{W}_i$. Therefore, as long as the fractures themselves are narrow on the length scale $\hat{x}_1$ of the current, it is consistent to treat them as 'point sinks', except possibly during a brief transient as the flow front first reaches a fracture: our emphasis will be on the longer-term dynamics, so we will neglect the details of this transient.

2.2. *Non-dimensionalization*

We define

$$x = \frac{\hat{x}}{\hat{x}_1}, \quad x_i = \frac{\hat{x}_i}{\hat{x}_1}, \quad h = \hat{h} \left(\frac{\hat{\beta}}{\hat{x}_1 \hat{q}} \right)^{1/2}, \quad t = \hat{t} \frac{(\hat{q}\hat{\beta})^{1/2}}{\hat{x}_1^{3/2}} \quad \text{and} \quad \lambda_i = \hat{\lambda}_i \frac{\hat{x}_1^{3/2}}{(\hat{q}\hat{\beta})^{1/2}}, \tag{2.6}$$

to eliminate $\hat{q}$, $\hat{\beta}$ and $\hat{x}_1$ and obtain the governing equation

$$\frac{\partial h}{\partial t} = \frac{\partial}{\partial x} \left(h \frac{\partial h}{\partial x} \right) \qquad \text{for} \qquad x \neq x_i, \tag{2.7}$$

together with the flux conditions at each sink

$$\left[h\frac{\partial h}{\partial x}\right]_{x_i-}^{x_i+} = \lambda_i h(x_i, t), \qquad \text{i.e.} \qquad \left[\frac{\partial h}{\partial x}\right]_{x_i-}^{x_i+} = \lambda_i \tag{2.8}$$

and the boundary condition $h\partial h/\partial x = -1$ at $x = 0$.

The sinks are located at x_i for $i = 1, 2, \ldots,$ with $x_1 = 1$. We will investigate how the spacing and strength of these sinks affects the spreading of the current, and in particular the possibilities for both steady-state and time-dependent behaviour.

3. A single fracture

We start by considering the behaviour of the current when there is a single fracture in its path. We will first look for steady-state solutions in which the current reaches the fracture and drains completely into it; we will then investigate the time-dependent problem numerically and analytically.

3.1. *Steady-state solutions*

In general, for a steady current carrying a constant uniform flux q, the current profile between sinks and sources obeys the equation

$$h\frac{\mathrm{d}h}{\mathrm{d}x} = -q, \qquad \text{with the general solution} \qquad h(x) = (A - 2qx)^{1/2}, \tag{3.1}$$

where A is a constant of integration to be determined. Steady solutions in the presence of multiple sinks and sources may be constructed by piecing together sections with this form, setting A and q in each region to satisfy the boundary and continuity conditions.

In particular, when there is a single sink of strength λ_1 located at $x = 1$, the steady state must satisfy $\lambda_1 (A - 2)^{1/2} = 1$, and thus

$$A = 2 + \frac{1}{\lambda_1^2}, \qquad \text{i.e.} \qquad h(x) = \left(2 + \frac{1}{\lambda_1^2} - 2x\right)^{1/2}. \tag{3.2}$$

Although the gradient and depth of the flow remain finite as $x \to 1_-$, if we postulate that the region beyond the fracture is 'dry' of intruding fluid then h must be discontinuous at the fracture. Such discontinuous profiles are unstable, because a slight perturbation leads to a high but finite gradient rather than a perfect discontinuity, and thus to flow which tends to eliminate the high-gradient region. This means that the steady-state solution presented above cannot quite be realized; however, as we will see below, it remains significant as an attractor of the time-dependent flow.

3.2. *Spreading before the first fracture*

Before the injectate reaches the first fracture, the attracting solution to (2.7) is the classic similarity solution with constant input flux (Huppert & Woods 1995). This solution is not available in closed form, but it may be written as

$$h(x, t) = t^{1/3} H(\eta), \quad \text{where} \quad \eta = \frac{x}{t^{2/3}} \quad \text{and} \quad \frac{1}{3}H - \frac{2}{3}\eta\frac{\mathrm{d}H}{\mathrm{d}\eta} = \frac{\mathrm{d}}{\mathrm{d}\eta}\left(H\frac{\mathrm{d}H}{\mathrm{d}\eta}\right). \tag{3.3}$$

The boundary conditions are that $H\mathrm{d}H/\mathrm{d}\eta = -1$ at $\eta = 0$ while $H = 0$ at some position $\eta = \eta_0$; the latter then requires that $\mathrm{d}H/\mathrm{d}\eta = -2\eta_0/3$ at $\eta = \eta_0$, and it is easy to use this as the initial condition for a numerical integration, and obtain η_0 by shooting. The shooting process gives $\eta_0 \approx 1.4819$ (and consequently $H(0) \approx 1.296$); we note that

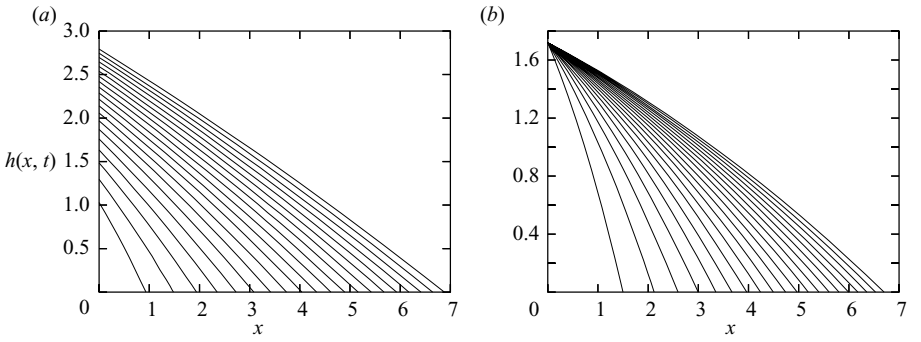

FIGURE 1. Similarity solutions $h(x,t)$ plotted at $t=0.5$ to 10 at intervals of 0.5, with (*a*) constant flux $q=1$ at $x=0$ and (*b*) decreasing flux $q=t^{-1/2}$ at $x=0$.

this means that the current reaches the first fracture at $t=t_1=(1/\eta_0)^{3/2}\approx 0.554$. The solution is plotted in figure 1(*a*), alongside a similarity solution for a decaying input flux, which we will require later.

3.3. *The quasi-steady 'leaking' state*

We now consider flow with a single fracture of strength λ_1 located at $x=1$. The unique steady-state solution in this case is given by equation (3.2) but, as noted above, we may expect this solution to be unstable; since no other steady state is available to attract the system, it is not obvious in advance what will occur. To investigate the behaviour of the system, the governing equations (2.7) and (2.8) were integrated numerically using the method described in Appendix (A).

Typical results are shown in figure 2, which illustrates the long-term evolution of the current for high and for low values of λ_1. The overall pattern is the same in each case. After the current reaches the fracture, it adjusts in the region $x<1$ towards the steady-state solution (3.2). The depth discontinuity at the fracture, however, is unsustainable, and ahead of the fracture a 'leakage current' develops. The leakage current is fed by the small 'leakage flux' of fluid which crosses the fracture; this fluid is able to cross the fracture because $h(1,t)$ is somewhat smaller than the steady-state depth $1/\lambda_1$, so the hydrostatically driven drainage rate is lower than the supplied flux. The leakage flux decreases gradually with time, as the depth at the fracture increases towards $1/\lambda_1$.

The further details of the current's evolution depend on λ_1. For a high value of λ_1 figures (2*a* and 2*b*), the flow in $x<1$ rapidly adjusts to be very close to the steady state given by (3.2); beyond $x>1$ the leakage current develops, fed by a small leakage flux, and spreads in an approximately self-similar manner which we will discuss further below. For a higher value of λ_1 (figures 2*c* and 2*d*), the depth and leakage flux at $x=1$ are very much greater. In $x<1$, the current adjusts first to a 'quasi-steady' state in which the flux is approximately constant in x but the depth is somewhat less than that predicted by (3.2); this part of the current then adjusts slowly towards the final steady state. Meanwhile, the leakage current spreads rapidly beyond $x=1$, gradually adjusting towards self-similar form as the depth deficiency $1/\lambda_1-h(1,t)$ becomes small.

We will now investigate the intermediate asymptotics of the leakage current. We seek an asymptotic description for $t\to\infty$, in which the current behind the fracture $(0<x<1)$ is steady at leading order, while the current beyond the fracture $(x>0)$ spreads at leading order according to a self-similar solution. We first note that this

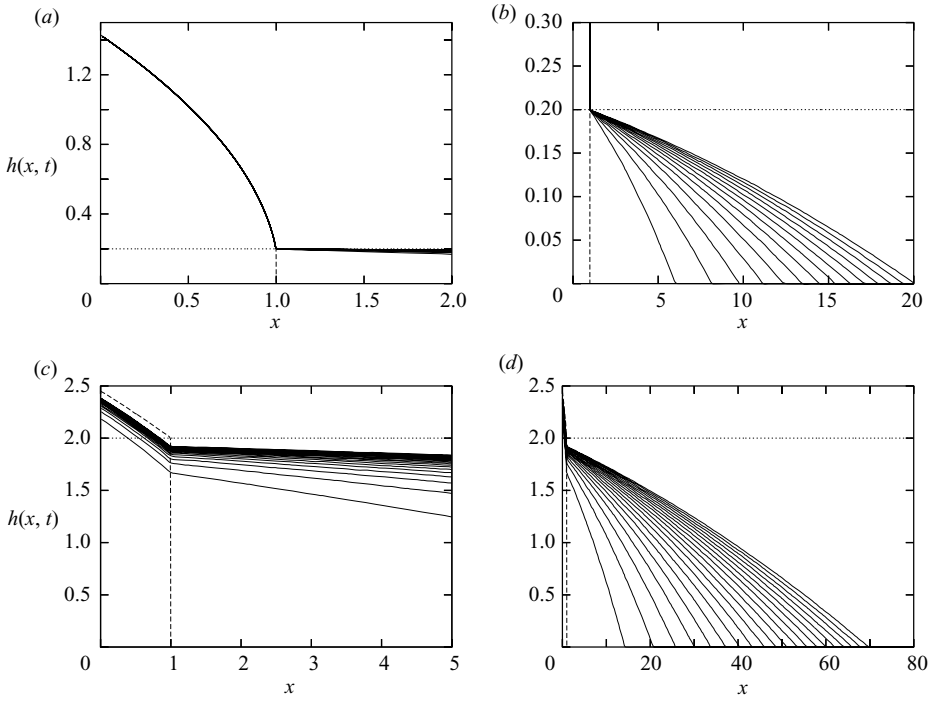

FIGURE 2. Numerical results for a single fracture: 'snapshots' of the current profile $h(x,t)$. In (*a*), (*b*) $\lambda_1 = 5$ and snapshots are taken at $t = 50$ to $t = 700$, at intervals of 50; in (*c*), (*d*) $\lambda_1 = 0.5$ and snapshots taken at $t = 50$ to $t = 1000$, at intervals of 50. The pairs (*a*, *b*) and (*c*, *d*) each show the same data over different ranges. The dashed lines mark the steady-state solution (3.2); the dotted lines mark the steady-state depth $1/\lambda_1$.

self-similar solution must have constant depth at its source, $x = 1$, and a consideration of the scalings in (2.7) then requires that it lengthens as $t^{1/2}$ and is fed by a flux which decays as $t^{-1/2}$. This motivates an asymptotic expansion in powers of $t^{-1/2}$,

$$h(x,t) = \begin{cases} h_{01}(x,t) & \text{for} \quad 0 < x < 1, \\ h_l(\xi,t) & \text{for} \quad x > 1, \end{cases} \tag{3.4}$$

where $\xi = (x-1)t^{-1/2}$, and where we define

$$h_{01}(x,t) = h_0(x) + \frac{1}{t^{1/2}}h_1(x) + \frac{1}{t}h_2(x) + \frac{1}{t^{3/2}}h_3(x) + O\left(\frac{1}{t^2}\right) \tag{3.5}$$

for $h_0(x) = (2 + 1/\lambda_1^2 - 2x)^{1/2}$, and

$$h_l(\xi,t) = H_0(\xi) + \frac{1}{t^{1/2}}H_1(\xi) + \frac{1}{t}H_2(\xi) + O\left(\frac{1}{t^{3/2}}\right). \tag{3.6}$$

The boundary conditions are, as before, the flux condition at $x = 0$, the continuity of depth and the jump condition in flux at $x = 1$, and the condition that flux vanishes at the front of the current $x = x_f(t)$. Following the numerical results (figure 2), we assume that this last condition will be met by setting $h = 0$ and $h\partial h/\partial x = 0$ at $x_f(t)$, as in previously published solutions for gravity currents in porous media.

Appendix B describes how the first few terms in these asymptotic expansions may be obtained: we omit the details here for clarity. (The key to the analysis is that the

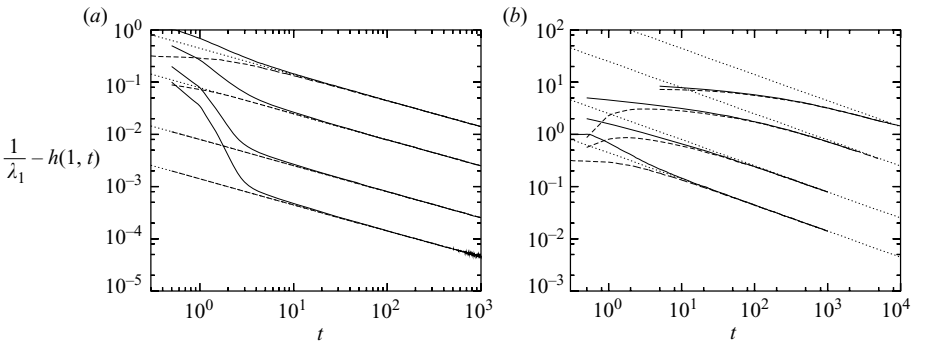

FIGURE 3. Depth deficiency $1/\lambda_1 - h(1,t)$, for (*a*) $\lambda_1 = 1$ (highest), 2, 5 and 10 (lowest); (*b*) $\lambda_1 = 0.1$ (highest), 0.2, 0.5 and 1 (lowest). The initial condition was either $h = 10^{-7}$ (solid lines) or the steady state (3.2) in $x < 1$ and $h = 10^{-7}$ in $x > 1$ (dashed lines). Dotted lines represent the asymptotic solution $1/\lambda_1 - h(1,t) \sim 0.444\lambda_1^{-5/2}t^{-1/2}$.

flux in $0 < x < 1$ is constant up to and including $O(t^{-1})$, and so it adjusts much more rapidly than the leakage current evolves: consequently, the depth at $x = 1$ adjusts rapidly towards $h = 1/\lambda_1$, and this depth sets the dynamics of the leakage current, which in turn controls the next-order corrections to the current in $0 < x < 1$.) We find that the front of the current advances as

$$x_f(t) \approx \frac{1.616}{\lambda_1^{1/2}} t^{1/2} - \frac{0.999}{\lambda_1^2} + O\left(\frac{1}{t^{1/2}}\right), \tag{3.7}$$

while the depth at the fracture is given by

$$h(1,t) \approx \frac{1}{\lambda_1} - \frac{0.444}{\lambda_1^{5/2}} \frac{1}{t^{1/2}} + \frac{1.60 \times 10^{-4}}{\lambda_1^4} \frac{1}{t} + O\left(\frac{1}{t^{3/2}}\right), \tag{3.8}$$

and the flux of fluid reaching the fracture from the left is given by

$$q(1_-,t) \approx 1 - \frac{0.222}{\lambda_1^{7/2}} \left[\left(2 + \frac{1}{\lambda_1^2}\right)^{1/2} - \frac{1}{\lambda_1}\right] \frac{1}{t^{3/2}} + O\left(\frac{1}{t^2}\right). \tag{3.9}$$

3.3.1. *Convergence to the asymptotic state*

We may quantify how the flow converges to the asymptotic solution derived above by examining the variation in time of the solution at $x = 1$. The most informative quantity to plot is the 'depth deficiency' $1/\lambda_1 - h(1,t)$, which reveals two regimes of behaviour (figures 3*a* and 3*b*).

For $\lambda_1 \gtrsim 1$ (figure 3*a*), convergence to the asymptotic solution is rapid, occurring over a time scale of order 1 which does not depend strongly on λ_1. Convergence in this regime is driven by the adjustment of the current in $0 < x < 1$, which to leading order 'sees' a boundary condition $h(1) = 0$ independently of λ, and adjusts over an $O(1)$ time scale to supply a flux $q(1_-,t) \approx 1$. This in turn allows the self-similar leakage current to be established rapidly. (Although the value of λ_1 is not important, the loss of fluid at $x = 1$ is: the time taken for adjustment is rather greater than 1, while the time taken for enough fluid to be injected to create the steady solution is given by $t \approx 0.94$: we see that because of the flux lost to the fracture, this is a considerable underestimate.)

For $\lambda_1 \lesssim 1$ (figure 3*b*), the convergence to the similarity solution is much slower, and the time required increases rapidly as λ_1 falls. This variation with λ_1 is consistent

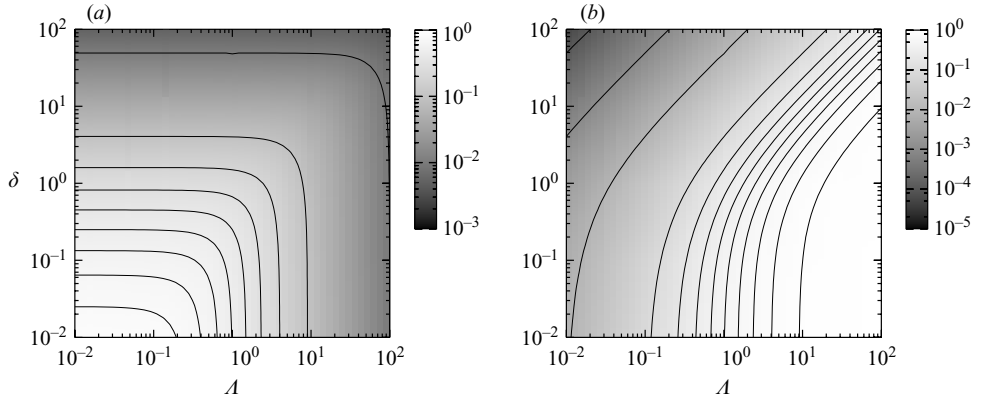

FIGURE 4. (*a*) The flux q_{12} between the two fractures: contours are at 0.01 (uppermost) and 0.1 to 0.8 in increments of 0.1. (*b*) The scaled depth at the second fracture, $\lambda_1 h(x_2)$: contours are at 10^{-4} (leftmost), 10^{-3}, 10^{-2} and 0.1 to 0.9 in increments of 0.1.

with the structure of the asymptotic expansion (3.8) for $h(1, t)$, in which the expansion variable is effectively $\lambda_1^{3/2} t^{1/2}$, so critical time scales will vary roughly with λ_1^{-3}. These results support the asymptotic expansion as a description of the long-time evolution of the current.

4. Two or more fractures

The steady-state and self-similar solutions obtained above give a reasonably complete description of what occurs when the current meets a single isolated fracture. In this section, we will consider what happens when it encounters two or more.

4.1. *Steady states for two fractures*

We first consider the situation where there is a second sink, of strength λ_2, at $x_2 > 1$. Ignoring all questions of stability for the moment, there is clearly one steady solution, derived above, in which the current reaches only to $x = 1$ and all drains through the first sink.

There is also a second solution in which the current reaches x_2 and drains partly through each sink. This is given by

$$h(x) = \begin{cases} h_{01} = (A_{01} - 2x)^{1/2} & \text{in} \quad 0 \leqslant x \leqslant 1, \\ h_{12} = (A_{12} - 2q_{12}x)^{1/2} & \text{in} \quad 1 \leqslant x \leqslant x_2. \end{cases} \tag{4.1}$$

By matching depths and fluxes at $x = 1$ and imposing the flux condition at $x = x_2$, we obtain the unique physically relevant solution

$$A_{01} = 2 + \frac{(1 - q_{12})^2}{\lambda_1^2} \qquad A_{12} = \frac{q_{12}\left(2x_2\lambda_2^2 + q_{12}\right)}{\lambda_2^2}, \qquad q_{12} = \frac{1 + \delta - \sqrt{\delta^2 + 2\delta + \Lambda^2}}{1 - \Lambda^2}, \tag{4.2}$$

where for convenience we have defined $\Lambda = \lambda_1/\lambda_2$ and $\delta = \lambda_1^2(x_2 - 1)$.

Figure 4(*a*) shows the variation of the flux q_{12} with the fracture strength ratio Λ and the scaled separation distance δ. As either the separation increases or the relative strength of the second fracture decreases, q_{12} decreases rapidly. In particular, we note that the second fracture can only consume more than half the current (i.e. $q_{12} > 1/2$) when $\delta < (1 - \Lambda^2)/4$; thus the majority of the fluid will always go down the first fracture if either $\Lambda \geqslant 1$ (i.e. $\lambda_1 \geqslant \lambda_2$) or $\delta \geqslant 1/4$ (i.e. $4(x_2 - 1) \geqslant \lambda_1^{-2}$). We also note

that it is only for very small Λ and δ that the condition $\lambda_1 h(x_1) \ll 1$ is satisfied, so outside this regime the point sink model remains valid (cf. § 2.1).

Figure 4(*b*) illustrates the depth of the current at the second fracture, $h(x_2)$, which controls the flux into the leakage current. It is convenient to plot $\lambda_1 h(x_2)$ (in other words the ratio of the downstream depth with two fractures to that with a single fracture), since we can write this as a function of Λ and δ only, $\lambda_1 h(x_2) = \Lambda q_{12}$. This rescaled downstream depth increases with increasing Λ, as the second fracture becomes weaker (so although less fluid is drawn beyond the first fracture, the depth at x_2 must increase to drive fluid through the second fracture, and it is this second effect which dominates). However, as the separation δ is increased, the reduction in q_{12} drives a corresponding reduction in $h(x_2)$. We note that the downstream depth is always reduced by adding a second fracture, and that across most of parameter space this decrease is quite substantial. This suggests that multiple fractures may be quite effective in trapping a current: we will return to this point below.

4.2. *Multiple fractures and continuously permeable regions of finite length*

Before considering the case of multiple fractures, it is helpful to consider a natural complement to the discrete-fracture problem. This occurs when the substrate is everywhere impermeable except for a region of finite length in which it is slightly permeable, so that fluid drains though it according to the 'slow drainage' model of PWH01. In this section we will recapitulate the results of PWH01 which are relevant to this situation; we will then discuss how it can be described as the limit of an array of discrete fractures.

We let the permeable region extend from $x = 0$ to $x = L$, with input flux q at $x = 0$, and the steady draining flow be described, following PWH01, by

$$\frac{\mathrm{d}}{\mathrm{d}x}\left(h\frac{\mathrm{d}h}{\mathrm{d}x}\right) = \lambda h. \tag{4.3}$$

We can rescale by defining $x' = x/L$, $h' = h/(Lq)^{1/2}$ and $\lambda' = \lambda L^{3/2}/q^{1/2}$ to obtain

$$\frac{\mathrm{d}}{\mathrm{d}x'}\left(h'\frac{\mathrm{d}h'}{\mathrm{d}x'}\right) = \lambda' h' \quad \text{in} \quad 0 < x' < 1, \qquad \text{with} \qquad h'\frac{\mathrm{d}h'}{\mathrm{d}x'} = -1 \quad \text{at} \quad x' = 0. \tag{4.4}$$

There are now two possible ways to achieve a steady state. One is for the current to drain out completely within the permeable region: for this to occur and for the solution to be stable, we must then have solutions for which $h' = 0$ at some finite $x' < 1$. Such a solution was derived by PWH01, and has the form

$$h'(x') = \frac{\lambda'}{6}\left(\frac{18^{1/3}}{\lambda'^{2/3}} - x'\right)^2 \qquad \text{in} \quad 0 < x' < \frac{18^{1/3}}{\lambda'^{2/3}}. \tag{4.5}$$

This solution can be realized in the finite fracture $x' < 1$ if $\lambda' > 18^{1/2} \approx 4.24$. For lower values of λ', it is not possible for the current to drain away completely, and we must seek a different class of solutions. These have the same form as the 'leakage currents' found for the discrete-fracture problem: within the permeable region, the current adjusts to a quasi-steady state in which at leading order in t the flux vanishes at the end of the fracture ($x' = 1$), but there is a slight depth-deficiency at $x' = 1$ which feeds a leakage current with a gradually decaying flux of fluid.

Continuity of flux requires the leading-order solution in the permeable region to satisfy $h'\mathrm{d}h'/\mathrm{d}x' = 0$ at $x' = 1$, and since for $\lambda' < 18^{1/2}$ we cannot satisfy this by setting $h'(1) = 0$, we must instead set $\mathrm{d}h'/\mathrm{d}x' = 0$ there. The resulting boundary value problem

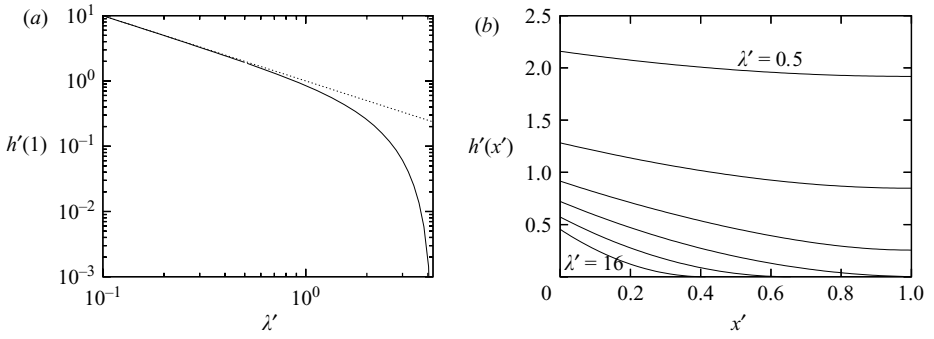

FIGURE 5. Steady solutions for flow over a permeable region: (*a*) downstream depth $h'(1)$ as a function of λ' (dotted line shows the asymptotic $h'(1) \sim 1/\lambda'$); (*b*) solutions $h'(x')$ for $\lambda' = 0.5$ (highest), 1, 2, 4, 8 and 16 (lowest).

is easy to solve numerically: it turns out that solutions are available precisely when $\lambda' < 18^{1/2}$, so this class of solutions complements those described by (4.5).

Figure 5(*a*) illustrates the variation of the depth $h'(1)$ of the current at the downstream end of the permeable region. For small λ', the depth varies as $1/\lambda'$, so as the drainage rate becomes small the finite length of the permeable region becomes irrelevant, and we approach the solution for a discrete fracture. Figure 5(*b*) shows the profiles $h'(x')$ of the current for a range of λ': as λ' reduces, the profile becomes increasingly flat, so as $\lambda' \to 0$ the drop in h' across the permeable region reduces towards zero.

The asymptotic description of the leakage current must be the same as that given in § B.2, with the difference that the depth is now set by $H_0(0) = (Lq)^{1/2} h'(1; \lambda')$ instead of simply by $H_0(0) = 1/\lambda_1$. (In the limit of slow drainage, when $h'(1; \lambda') = 1/\lambda'$, we have $H_0(0) = q/(\lambda L)$: as we might expect, this agrees with the discrete-fracture model for $q = 1$ if we take $\lambda_1 = \lambda L$.)

4.2.1. *The continuously permeable region as the limit of many discrete fractures*

It is natural to expect that a large array of discrete fractures will be similar in effect to a continuously permeable region covering the same area. The simplest case is when we consider a sequence of evenly spaced fractures of equal strength. We let the fractures be positioned at $x'_i = i/N$ for $i = 1, \ldots, N$ and have strength $\lambda_i = \lambda/N$. In the region $x'_{i-1} \leqslant x' \leqslant x'_i$, following (3.1) we let $h(x') = (A_i - 2q_i(x' - x'_{i-1}))^{1/2}$: matching depths and fluxes at each fracture yields

$$\left(A_i - \frac{2q_i}{N}\right)^{1/2} = A_{i+1}^{1/2} \quad \text{and} \quad q_i - \frac{\lambda}{N} A_{i+1}^{1/2} = q_{i+1} \quad \text{for} \quad i = 1, \ldots, N = 1. \tag{4.6}$$

We also have the boundary conditions $q_1 = 1$ and

$$q_N = \frac{\lambda}{N}\left(A_N - \frac{2q_N}{N}\right)^{1/2}, \quad \text{i.e.} \quad q_N = -\frac{\lambda^2}{N^3} + \frac{\lambda^2}{N^3}\left(1 + \frac{N^4 A_N}{\lambda^2}\right)^{1/2}. \tag{4.7}$$

It is simplest to write this system in a form which allows us to solve 'backwards' starting from A_N: we can then obtain a single equation for A_N such that $q_1 = 1$. We obtain the difference equations

$$q_i = \frac{\lambda}{N} A_{i+1}^{1/2} + q_{i+1} \quad \text{and} \quad A_i = \frac{2}{N}\left(\frac{\lambda}{N} A_{i+1}^{1/2} + q_{i+1}\right) + A_{i+1}. \tag{4.8}$$

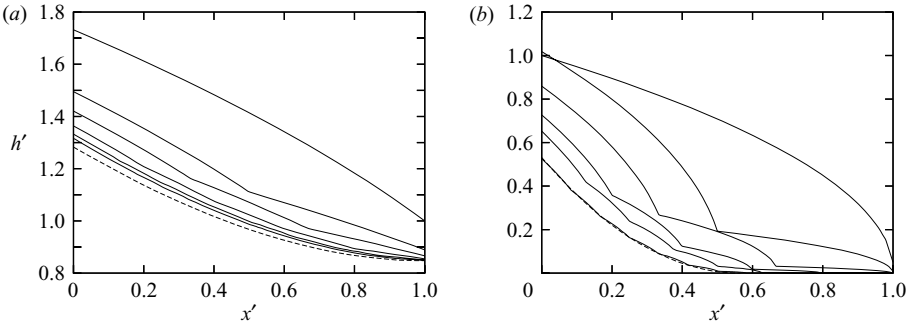

FIGURE 6. Steady solutions for flow over a permeable region: (*a*) the solution $h'(x')$ for $\lambda' = 1$ (dashed) compared with the corresponding solutions for 12, 8, 5, 3, 2, and 1 discrete fractures; (*b*) the solution $h'(x')$ for $\lambda' = 10$ (dashed) compared with the corresponding solutions for 12, 8, 5, 3, 2, and 1 discrete fractures.

We cannot solve this set of difference equations in closed form, but we can show that solutions must exist: we have $q_1 \geqslant A_N^{2-N}$ (which is an increasing and unbounded function of A_N for any finite N); furthermore, when $A_N = 0$, $q_i = 0$ for all $i < N$. We deduce that for any finite N and any value of λ there must always be a solution for A_N such that the condition $q_1 = 1$ is satisfied.

Some typical profiles are shown in figure 6. As N increases, the difference equations (4.8) model the differential equation (4.4) increasingly closely, and the steady-state profiles given piecewise by (3.1) collapse onto the profiles for continuous permeability plotted in figure 5. We note that this collapse occurs both for $\lambda' < 18^{1/2}$ (figure 6*a*), when the continuous solution has finite depth at $x' = 1$, and for $\lambda' > 18^{1/2}$ (figure 6*b*), when the continuous solution vanishes before $x' = 1$. In the latter case, the depth of the piecewise solutions decreases rapidly with increasing N in the region beyond the front of the continuous current, but they never entirely vanish.

The piecewise solutions converge fairly rapidly to the continuous solution as N increases. We note that as N increases the depth at $x' = 1$ decreases, reaching its minimum in the continuum limit. Recalling that the leakage flux increases with increasing depth at the downstream end of the fracture, we conclude that a continuously permeable region is more effective at trapping an oncoming current than are the corresponding set of discrete fractures. This trend is stronger for higher values of λ' (recall that as $\lambda' \to 0$, the values of $h'(1)$ predicted by the continuum model and by the single-fracture model are both given asymptotically by $1/\lambda'$).

4.3. *Numerical results for time-dependent flow*

We have carried out a series of numerical integrations to confirm the accuracy of the picture obtained above. Figure 7 shows the results of a series of numerical integrations comparing the system with continuous drainage with an 'equivalent' set of discrete fractures. In each case, the region of continuous drainage was taken to lie between $x = 1$ and $x = 2$, and the discrete fractures were located at $x_i = 1 + i/N$ for $i = 1, \ldots, N$.

Figures 7(*a*) and 7(*c*) show a case, $\lambda = 1$, in which the continuously permeable region is unable to trap the current. The downstream depth $h(2)$ in the steady state is quite large, and so a large leakage current is supplied, while the current in the region $x < 2$ has adjusted to almost its final steady state by the time the first plotted 'snapshot' is taken. There is only a very small difference between the continuous-drainage current

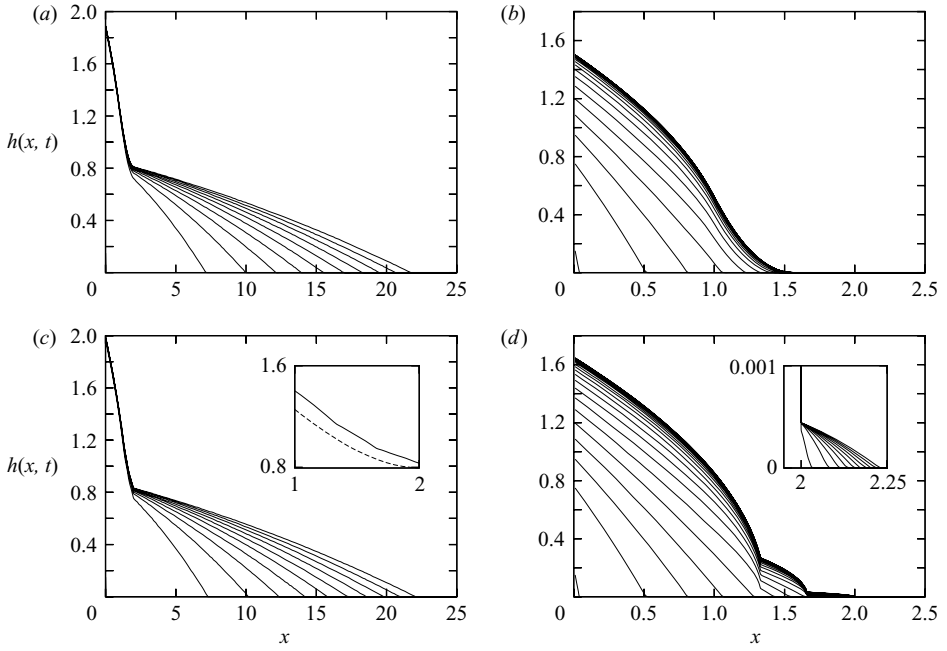

FIGURE 7. Numerical results for multiple fractures or continuously permeable regions. (*a*) Profiles for $\lambda = 1$: snapshots at $t = 20$ to $t = 200$ at intervals of 20. (*b*) Profiles for $\lambda = 10$: snapshots at $t = 0$ to $t = 5$ at intervals of 0.2. (*c*) Profiles for $\lambda = 1$ and $N = 3$: snapshots at $t = 20$ to $t = 200$ at intervals of 20; inset compares profiles at $t = 200$ for discrete-fracture case (solid) and continuously draining case (dashed). (*d*) Profiles for $\lambda = 10$ and $N = 3$: main panel shows snapshots at $t = 0$ to $t = 5$ at intervals of 0.2; inset shows snapshots at $t = 0$ to $t = 50$ at intervals of 5.

(figure 7*a*) and the current with three discrete fractures (figure 7*c*): the latter is slightly deeper, as the inset in figure 7(*c*) indicates, and the leakage current is correspondingly slightly larger. Comparison with figure 6 indicates that by $t = 200$ the solutions in $1 < x < 2$ are extremely close to their final quasi-steady state.

Figures 7(*b*) and 7(*d*) show a case, $\lambda = 10$, in which the continuously permeable region is able to trap the current. Figure 7(*b*) therefore shows no leakage current, in contrast to the case of three discrete fractures (figure 7*d*), where there is a (very small) leakage current beyond $x = 2$. Again, comparison with figure 6 indicates that by $t = 5$ the solutions in $1 < x < 2$ have become extremely close to their final quasi-steady state, and that the quasi-steady current with discrete fractures is slightly deeper than that with continuous drainage.

In summary, these numerical integrations of the time-dependent model confirm that the steady-state and leakage current analysis captures the behaviour of the flow across multiple fractures.

5. Discussion and conclusions

We have presented a number of exact, asymptotic and numerical solutions which describe the spreading of constantly fed gravity currents in a porous medium, when the otherwise impermeable substrate along which they flow is punctuated either by one or more short but highly permeable fractures or by a continuous region of low but non-zero permeability. A key question is whether such fractures can 'trap' a

current entirely, or whether some fluid is able to pass beyond them. We find that a continuously permeable region is able to trap the current completely when the rescaled drainage parameter $\lambda' = \lambda L^{3/2}/q^{1/2}$ is greater than $18^{1/2}$. In all other circumstances, both for discrete and continuous sinks, the model admits steady solutions in which the current is completely trapped, but these solutions are not stable. Rather, they describe a quasi-steady state towards which the current adjusts asymptotically; however, a small flux of fluid is able to bypass the fractured region in each case. This flux diminishes asymptotically as $t^{-1/2}$, and the leakage current which it feeds lengthens asymptotically as $t^{1/2}$. The coefficient in this spreading law depends on the depth of the steady-state solution at the downstream end of the fracture, so the quasi-steady balance between supply and drainage acts as a 'hydrostatic control' which determines the properties of the leakage current. These asymptotic descriptions are of most use when the current is 'nearly trapped', so that the drainage flux is indeed small. Numerical integrations of the model for single and multiple fractures and for a continuously permeable region confirm the picture built up analytically.

These drainage-affected gravity currents have some interesting features. One is the emergence of a current which spreads as $t^{1/2}$ rather than the more familiar $t^{2/3}$ of a constant-flux current or $t^{1/3}$ of a constant-volume current (Huppert & Woods 1995). Another notable feature is that although the steady-state solutions are unstable, they provide a good description of the current at long times everywhere except the region beyond the last fracture; this thus enables estimates to be made easily of the eventual drainage pattern of the current. A final feature which should be pointed out is the rapid convergence as N increases of the multiple-fracture solutions to the continuous-drainage solution in both regimes $\lambda' \gtrless 18^{1/2}$: this supports the earlier modelling work of PWH01 as a simple and tractable description of drainage through a multiply fractured substrate.

These results suggest that in practical situations (for example the management of aquifer recharge or pollutant sequestration schemes), it may be possible to deduce the principal features of the horizontal and vertical spreading of injected fluid by carrying out steady-state, rather than fully time-dependent, calculations, with consequent savings in computational resources. Meanwhile, they suggest that the complete trapping of a current by fractures may be difficult to achieve, especially if there is a small number of relatively large fractures rather than an array of many small fractures. In these circumstances, monitoring for leakage currents beyond the fractured region may be necessary even if the fractured region is large enough, in principle, to swallow the current entirely.

A particularly interesting possibility occurs if we consider the injection of fluid into a laterally unconfined porous layer where there is a localized fractured region of substrate close to the point of injection. (For example, we might consider injection into an aquifer where a new injection well is sunk near to an abandoned production well: this problem is similar to those considered by Nordbotten *et al.* (2004), with the difference that we do not assume that the fluid occupies the whole depth of the horizontal layer.) In this case, in contrast to the present study, the flow is essentially two-dimensional. If drainage through the fracture is neglected, we may expect the injectate to spread radially, with radius $\hat{r} \propto (\hat{\beta}\hat{q})^{1/4}\hat{t}^{1/2}$ and maximum depth $\hat{h} \propto (\hat{q}/\hat{\beta})^{1/2}$ independent of $\hat{t}$ at the point of injection (Lyle *et al.* 2005; Bickle *et al.* 2007). Extending the principle of our one-dimensional results to this situation, we might expect that the depth near the point of injection and the fracture will in fact be controlled hydrostatically by a leading-order balance between injection and drainage, while the current spreads at large distances according to a similarity solution with fixed

depth at the source (so radius increases as $t^{1/2}$, though with a different coefficient to that found for the constant-flux current without leakage). Thus the spreading current, imaged in a horizontal plane, might appear on first inspection to be spreading across an impermeable substrate when in reality it is leaking into regions above (in the case of buoyant fluid) or below. This illustrates a potential difficulty in interpreting observations of the spreading of injectates in fractured or otherwise heterogeneous porous media.

I would like to thank Professor Andy Woods for helpful and encouraging discussions on this work, and also three anonymous referees for their useful comments. Much of this work was carried out at the BP Institute for Multiphase Flow, University of Cambridge, and supported financially by a postdoctoral fellowship under the NERC/EPSRC EMS scheme (ref. NE/B50188X/1).

Appendix A. Numerical method

The nonlinear diffusion equation (2.7) was integrated numerically using an implicit time- and space-centred differencing scheme, following Press *et al.* (1992, § 19.2). Spatially one-sided estimates were used for the derivatives close to the sinks $x = x_i$ for accuracy where $\partial h/\partial x$ is expected to be discontinuous, along with a higher-order volume estimate for h at this point. Combining these difference equations and the corresponding equations for the trivial boundary conditions at the ends of the domain gives a tridiagonal system to solve at each time step; this was done using the `tridag` routine of Press *et al.* (1992).

The scheme was implemented in Fortran 77. The typical grid resolution was $\Delta x = 0.005$ to 0.1 and $\Delta t = 0.0005$ to 0.05. All the results presented were robust to changes in resolution, and typical run-times on a 400 MHz Unix workstation were of the order of tens of seconds to tens of minutes.

Appendix B. Details of the asymptotic analysis for a single fracture

B.1. *Adjustment of the current behind the fracture*

We first consider the region $0 < x < 1$. The solution must obey equation (2.7), subject to the condition $h\partial h/\partial x = -1$ at $x = 0$ and to the flux and depth matching conditions at $x = 1$. Substituting the expansion (3.5) into (2.7), we find

$$-\frac{h_1(x)}{2t^{3/2}} - \frac{h_2(x)}{t^2} - \frac{3h_3(x)}{2t^{5/2}} = \frac{1}{2}\frac{\partial^2}{\partial x^2}\left[\left(h_0(x) + \frac{h_1(x)}{t^{1/2}} + \frac{h_2(x)}{t} + \frac{h_3(x)}{t^{3/2}}\right)^2\right] + O\left(\frac{1}{t^2}\right). \tag{B 1}$$

Since the right-hand side of this equation is simply the x-derivative of the fluid flux, this flux must be constant along the current up to order $t^{-3/2}$: hence the flux which reaches $x = 1$ adjusts to its quasi-steady value of $q = 1$ over a shorter time scale than that over which the leakage current spreads.

Carrying out the expansion and equating powers of t, we obtain a succession of equations and boundary conditions. The first two may be integrated immediately to give

$$h_1(x) = \frac{A_1}{h_0(x)} \qquad \text{and} \qquad h_2(x) = \frac{A_2}{2h_0(x)} - \frac{A_1^2}{2h_0^3(x)}, \tag{B 2}$$

where A_1 and A_2 are constants to be determined by the boundary condition at $x=1$ (and thus by the dynamics of the leakage current). At the next order in t, we obtain

$$\frac{\mathrm{d}^2}{\mathrm{d}x^2}\left[h_0(x)h_3(x)+h_1(x)h_2(x)\right]=-\frac{1}{2}h_1 \quad \text{with} \quad \frac{\mathrm{d}}{\mathrm{d}x}\left[h_0(x)h_3(x)+h_1(x)h_2(x)\right]\Big|_{x=0}=0, \tag{B 3}$$

and it is straightforward to integrate this to obtain

$$h_3(x)=-\frac{A_1}{6}h_0^2(x)+\frac{A_1}{4}\left(2+\frac{1}{\lambda_1^2}\right)^{1/2}h_0(x)+\frac{A_3}{h_0(x)}-\frac{A_1A_2}{2h_0^3(x)}+\frac{A_1^3}{2h_0^5(x)}, \tag{B 4}$$

where A_3 is another constant of integration.

At the upstream side of the fracture, where $x=1$ and $h_0=1/\lambda_1$, the conditions are

$$h(1_-,t)=\frac{1}{\lambda_1}+A_1\lambda_1\frac{1}{t^{1/2}}+\left(\frac{A_2\lambda_1}{2}-\frac{A_1^2\lambda_1^3}{2}\right)\frac{1}{t} + \left[-\frac{A_1}{6\lambda_1^2}+\frac{A_1}{4\lambda_1}\left(2+\frac{1}{\lambda_1^2}\right)^{1/2}+A_3\lambda_1-\frac{A_1A_2\lambda_1^3}{2}+\frac{A_1^3\lambda_1^5}{2}\right]\frac{1}{t^{3/2}}+O\left(\frac{1}{t^2}\right) \tag{B 5}$$

and

$$q(1_-,t)=1-\frac{A_1}{2}\left[\left(2+\frac{1}{\lambda_1^2}\right)^{1/2}-\frac{1}{\lambda_1}\right]\frac{1}{t^{3/2}}+O\left(\frac{1}{t^2}\right). \tag{B 6}$$

We will write these as, respectively,

$$h(1_-,t)=\frac{1}{\lambda_1}+\frac{B_1}{t^{1/2}}+\frac{B_2}{t}+\ldots \qquad \text{and} \qquad q(1_-,t)=1-\frac{Q_3}{t^{3/2}}+\ldots \tag{B 7}$$

B.2. *Behaviour of the leakage current*

We now consider the region $x>1$. Substituting (3.6) into (2.7) and expanding, we obtain the governing equations for the leading-order and first correction terms,

$$-\frac{1}{2}\xi\frac{\mathrm{d}H_0}{\mathrm{d}\xi}=\frac{\mathrm{d}}{\mathrm{d}\xi}\left(H_0\frac{\mathrm{d}H_0}{\mathrm{d}\xi}\right) \qquad \text{and} \qquad -\frac{1}{2}\frac{\mathrm{d}}{\mathrm{d}\xi}\left(\xi H_1\right)=\frac{\mathrm{d}^2}{\mathrm{d}\xi^2}\left(H_1H_0\right). \tag{B 8a, b}$$

Expanding the conditions for the continuity of depth and flux across the fracture, we obtain the corresponding boundary conditions,

$$H_0(0)=\frac{1}{\lambda_1}, \quad \lambda_1B_1=\left.H_0\frac{\mathrm{d}H_0}{\mathrm{d}\xi}\right|_0; \qquad H_1(0)=B_1, \quad \lambda_1B_2=\left.\frac{\mathrm{d}(H_0H_1)}{\mathrm{d}\xi}\right|_0. \tag{B 9a, b}$$

To expand the boundary conditions at the nose, we define $\xi_f=x_f(t)/t^{1/2}$, and expand this as $\xi_f=\xi_{f0}+\xi_{f1}t^{-1/2}+O(t^{-1})$. The condition $H(x_f,t)=0$ then gives at $O(1)$ and at $O(t^{-1/2})$ the conditions

$$H_0(\xi_{f0})=0 \qquad \text{and} \qquad H_0'(x_{f0})\xi_{f1}+H_1(\xi_{f0})=0. \tag{B 10a, b}$$

To impose the flux condition $\lim_{x\to x_f}H\partial H/\partial x=0$, we define $Z=1-(x-1)/x_f(t)$, and postulate an expansion of the form $h(Z,t)=\eta(t)Z+O(Z^2)$ for small Z; we obtain the condition that

$$\eta(t)=x_f(t)\frac{\mathrm{d}x_f}{\mathrm{d}t}, \qquad \text{i.e.} \qquad -\frac{1}{t^{1/2}}\left.\frac{\partial H}{\partial\xi}\right|_{\xi_f}=\frac{\mathrm{d}x_f}{\mathrm{d}t}. \tag{B 11}$$

Expanding this in powers of $t^{-1/2}$, the first two equations we obtain are

$$\left.\frac{\mathrm{d}H_0}{\mathrm{d}\zeta}\right|_{\xi_{f0}} = -\frac{1}{2}\xi_{f0} \qquad \text{and} \qquad \left[\frac{\mathrm{d}H_1}{\mathrm{d}\xi}+\xi_{f1}\frac{\mathrm{d}^2H_0}{\mathrm{d}\xi^2}\right]_{\xi_{f0}} = 0. \tag{B 12a, b}$$

We now have fully specified eigenvalue problems to solve for the functions $H_i(\xi)$ and the coefficients B_i and ξ_{fi}. We will consider only the first two terms in the expansion, as this is sufficient to confirm this solution is consistent with that established in $0 < x < 1$.

The leading-order problem is defined by equation (B 8*a*) together with the boundary conditions (B 9*a*), (B 9*b*), (B 10*a*) and (B 12*a*). Here B_1 and ξ_{f0} are solution parameters: we have a second-order system with four boundary conditions, which should be sufficient to determine them both.

For simplicity, we write the input flux as $-\lambda_1 B_1 = Q$. It is useful to eliminate Q by defining $\xi = Q^{1/3}\chi$, $\xi_{f0} = Q^{1/3}\chi_0$ and $H_0 = Q^{2/3}\Theta(\chi)$, and then to introduce the variable $\zeta = 1 - \chi/\chi_0$ to obtain

$$\frac{1}{2}(1-\zeta)\frac{\mathrm{d}\Theta}{\mathrm{d}\zeta} = \frac{1}{\chi_0^2}\frac{\mathrm{d}}{\mathrm{d}\zeta}\left(\Theta\frac{\mathrm{d}\Theta}{\mathrm{d}\zeta}\right) \tag{B 13}$$

with the boundary conditions

$$\Theta(0) = 0 \quad \text{and} \quad \left.\frac{\mathrm{d}\Theta}{\mathrm{d}\zeta}\right|_0 = \frac{1}{2}\chi_0^2; \qquad \Theta(1) = \frac{1}{Q^{2/3}\lambda_1} \quad \text{and} \quad \Theta\left.\frac{\mathrm{d}\Theta}{\mathrm{d}\chi}\right|_1 = \chi_0. \tag{B 14}$$

We now have a well-characterized shooting problem to solve, integrating from $\zeta = 0$ and varying χ_0 until the condition on $\mathrm{d}\Theta/\mathrm{d}\chi$ is satisfied at $\zeta = 1$. This may be done readily using Maple: we find that $\chi_0 \approx 2.119$, and that $\Theta = \Theta_0 \approx 1.719$ and $\mathrm{d}\Theta/\mathrm{d}\zeta = \Theta_1 \approx 1.233$ at $\zeta = 1$. The last of our boundary conditions now determines the unknown Q: we find

$$\Theta_0 = \frac{1}{Q^{2/3}\lambda_1}, \qquad \text{i.e} \qquad Q = \frac{1}{(\lambda_1\Theta_0)^{3/2}}. \tag{B 15}$$

In terms of our unknowns B_1 and A_1, this may be written as

$$B_1 = -\frac{Q}{\lambda_1} = -\frac{1}{\lambda_1^{5/2}\Theta_0^{3/2}}, \qquad \text{i.e.} \qquad A_1 = -\frac{1}{\lambda_1^{7/2}\Theta_0^{3/2}}. \tag{B 16}$$

We have now obtained the complete leading-order description of the current, in which it is steady behind the fracture and has a self-similar leakage current in front of the fracture. As λ_1 increases, so the fracture becomes more strongly draining, the depth at the fracture adjusts more rapidly towards its steady value, while the flux supplying the leakage current decreases in strength. The similarity solution, $H_0(\xi)$, is plotted in figure 1(*b*), alongside the solution for constant flux, figure 1(*a*); it is also interesting to compare the numerically obtained leakage currents in figures 2(*b*) and 2(*d*).

The next-order term, $H_1(\xi)$, must satisfy equation (B 8*b*) with the boundary conditions (B 9*d*), (B 10*b*), (B 12*b*) and, from (B 9*c*), $H_1(0) = -\lambda_1^{-5/2}\Theta_0^{-3/2}$. We can simplify these somewhat. First, we note that by expanding equation (B 13) around $\zeta = 0$, we can obtain $\mathrm{d}^2\Theta/\mathrm{d}\zeta^2 = -\chi_0^2/8$ and so $\mathrm{d}^2H_0/\mathrm{d}\xi^2 = -1/8$ at $\zeta = 0$. The boundary conditions at ξ_{f0} therefore simplify to $H_1(\xi_{f0}) = \xi_{f0}\xi_{f1}/2$ and $H_1'(\xi_{f0}) = \xi_{f1}/8$. We can also expand the condition (B 9*d*) to obtain

$$Q^{2/3}\Theta_0\frac{\mathrm{d}H_1}{\mathrm{d}\xi} + H_1\left[-\frac{Q^{1/3}}{\Theta_0}\right] = \lambda_1 B_2. \tag{B 17}$$

We rescale the equations, as before, by defining $H_0 = Q^{2/3}\Theta$, $H_1 = Q^{2/3}\Theta_1$, $\xi = Q^{1/3}\chi$, $\xi_{f1} = Q^{1/3}\chi_1$, and finally $\zeta = 1-\chi/\chi_0$; and we eliminate χ_1 from the shooting problem by defining $\Theta_1(\zeta) = \chi_1\beta(\zeta)$. We obtain

$$\frac{1}{2}\frac{\mathrm{d}}{\mathrm{d}\zeta}\left[(1-\zeta)\beta\right] = \frac{1}{\chi_0^2}\frac{\mathrm{d}^2}{\mathrm{d}\zeta^2}\left[\Theta\beta\right] \tag{B 18}$$

with

$$\beta = \frac{1}{2}\chi_0 \quad \text{and} \quad \frac{\mathrm{d}\beta}{\mathrm{d}\zeta} = -\frac{1}{8}\chi_0 \quad \text{at} \quad \zeta = 0;$$

$$\beta = -\frac{1}{\chi_1\lambda_1^{3/2}\Theta_0^{1/2}} \quad \text{and} \quad \frac{\mathrm{d}\beta}{\mathrm{d}\zeta} = \frac{\chi_0}{\chi_1\lambda_1^{3/2}\Theta_0^{5/2}} - \frac{B_2\lambda_1^{5/2}\chi_0\Theta_0^{1/2}}{\chi_1} \quad \text{at} \quad \zeta = 1. \tag{B 19}$$

Integrating the equation numerically to find $\beta(\zeta)$, and using the value of χ_0 obtained above, we obtain $\beta = \beta_0 \approx 0.5823$ and $\mathrm{d}\beta/\mathrm{d}\zeta = \beta_1 \approx -0.4175$ at $\zeta = 1$. Thus we have $\Theta_1 = \beta_0\chi_1$ and $\Theta_1' = \beta_1\chi_1$ at $\zeta = 1$, and we can use the boundary conditions at $\zeta = 1$ to write

$$\chi_1 = -\frac{1}{\lambda_1^{3/2}\Theta_0^{1/2}\beta_0} \quad \text{and} \quad B_2 = \frac{\beta_1}{\lambda_1^4\chi_0\Theta_0\beta_0} + \frac{1}{\lambda_1^4\Theta_0^3}. \tag{B 20}$$

REFERENCES

Acton, J. M., Huppert, H. E. & Worster, M. G. 2001 Two-dimensional viscous-gravity currents flowing over a deep porous medium. *J. Fluid Mech.* **440**, 359–380.

Bachu, S. 2000 Sequestration of CO_2 in geological media: criteria and approach for site selection in response to climate change. *Energy Conversion and Management* **41**, 953–970.

Barenblatt, G. I. 2003 *Scaling*. Cambridge University Press.

Bear, J. 1972 *Dynamics of Fluids in Porous Media*. Dover.

Bickle, M., Chadwick, A., Huppert, H. E., Hallworth, M. & Lyle, S. 2007 Modelling carbon dioxide accumulation at Sleipner: Implications for underground carbon storage. *Earth Planetary Sci. Lett.* **255**, 164–176.

Huppert, H. E. 1982 The propagation of two-dimensional and axisymmetric viscous gravity currents over a rigid horizontal surface. *J. Fluid Mech.* **121**, 43–58.

Huppert, H. E. & Woods, A. W. 1995 Gravity-driven flows in porous layers. *J. Fluid Mech.* **292**, 55–69.

King, S. E. & Woods, A. W. 2003 Dipole solutions for viscous gravity currents: theory and experiments. *J. Fluid Mech.* **483**, 91–109.

Latil, M. 1980 *Enhanced Oil Recovery*. Éditions Technip.

Lyle, S., Huppert, H. E., Hallworth, M., Bickle, M. & Chadwick, A. 2005 Axisymmetric gravity currents in a porous medium. *J. Fluid Mech.* **543**, 293–302.

Nordbotten, J. M., Celia, M. A. & Bachu, S. 2004 Analytical solutions for leakage rates through abandoned wells. *Wat. Resour. Res.* **40** (4), W04204, doi:10.1029/2003WR002997.

Press, W. H., Teukolsky, S. A., Vetterling, W. T. & Flannery, B. P. 1992 *Numerical Recipes in Fortran 77*, 2nd edn. Cambridge University Press.

Pritchard, D. & Hogg, A. J. 2002 Draining viscous gravity currents in a vertical fracture. *J. Fluid Mech.* **459**, 207–216.

Pritchard, D., Woods, A. W. & Hogg, A. J. 2001 On the slow draining of a gravity current moving through a layered permeable medium. *J. Fluid Mech.* **444**, 23–47.

Woods, A. W. 1998 Vaporizing gravity currents in a permeable rock. *J. Fluid Mech.* **377**, 151–168.